AD-A180 234 DLTS ANALYSIS AND MODELING OF ELECTRON AND PROTON IRRADIATED (ALGA)AS/GAA.. (U) FLORIDA UNIV GAINESVILLE DEPT OF ELECTRICAL ENGINEERING S S LI MAR 87 1/1

UNCLASSIFIED AFWAL-TR-86-2120 F33615-81-C-2058 F/G 7/2 NL

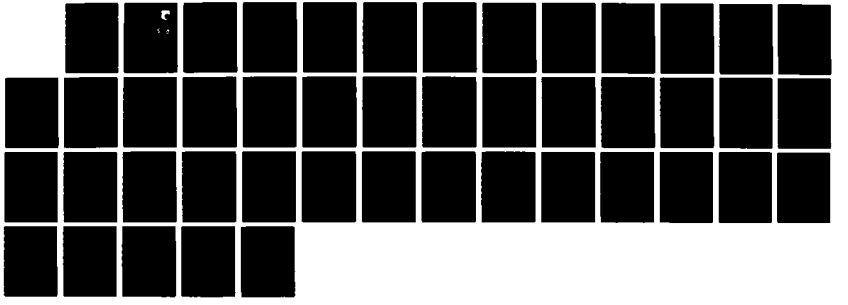

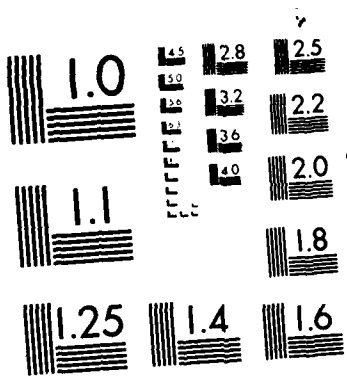

(12)

DTIC FILE COPY

AD-A180 234

AFWAL-TR-86-2120

DLTS ANALYSIS AND MODELING OF ELECTRON AND PROTON IRRADIATED (AlGa)As/GaAs MULTIJUNCTION SOLAR CELLS

Sheng S. Li

University of Florida
Department of Electrical Engineering
Gainesville, FL 32611

March 1987

Final Report for Period October 1985 - November 1986

Approved for public release; distribution is unlimited

AERO PROPULSION LABORATORY
AIR FORCE WRIGHT AERONAUTICAL LABORATORIES
AIR FORCE SYSTEMS COMMAND
WRIGHT-PATTERSON AIR FORCE BASE, OHIO 45433-6563

NOTICE

When Government drawings, specifications, or other data are used for any purpose other than in connection with a definitely related Government procurement operation, the United States Government thereby incurs no responsibility nor any obligation whatsoever; and the fact that the government may have formulated, furnished, or in any way supplied the said drawings, specifications, or other data, is not to be regarded by implication or otherwise as in any manner licensing the holder or any other person or corporation, or conveying any rights or permission to manufacture use, or sell any patented invention that may in any way be related thereto.

This report has been reviewed by the Office of Public Affairs (ASD/PA) and is releasable to the National Technical Information Service (NTIS). At NTIS, it will be available to the general public, including foreign nations.

This technical report has been reviewed and is approved for publication.

MICHAEL A. CHUNG, 2Lt, USAF
Project Engineer
Photovoltaics
Power Components Branch

Paul R. Bertheaud

PAUL R. BERTHEAUD, Chief
Power Components Branch
Aerospace Power Division

FOR THE COMMANDER

JAMES D. REAMS, Chief
Aerospace Power Division
Aero Propulsion Laboratory

If your address has changed, if you wish to be removed from our mailing list, or if the addressee is no longer employed by your organization please notify AFWAL/POOC, *W-PAFB, OH 45433 to help us maintain a current mailing list.*

Copies of this report should not be returned unless return is required by security considerations, contractual obligations, or notice on a specific document.

SECURITY CLASSIFICATION OF THIS PAGE

AD-A180 234

REPORT DOCUMENTATION PAGE

1a REPORT SECURITY CLASSIFICATION: Unclassified	1b RESTRICTIVE MARKINGS
2a SECURITY CLASSIFICATION AUTHORITY	3 DISTRIBUTION/AVAILABILITY OF REPORT: Approved for public release; distribution unlimited
2b DECLASSIFICATION/DOWNGRADING SCHEDULE	
4 PERFORMING ORGANIZATION REPORT NUMBER(S)	5 MONITORING ORGANIZATION REPORT NUMBER(S): AFWAL-TR-86-2120
6a NAME OF PERFORMING ORGANIZATION: University of Florida; 6b OFFICE SYMBOL (If applicable)	7a NAME OF MONITORING ORGANIZATION: Aero Propulsion Laboratory (AFWAL/POOC) AF Wright Aeronautical Laboratories (AFSCR)
6c ADDRESS (City, State and ZIP Code): Gainesville, Florida 32611	7b ADDRESS (City, State and ZIP Code): Wright-Patterson Air Force Base, Ohio, 45433-6563
8a NAME OF FUNDING/SPONSORING ORGANIZATION; 8b OFFICE SYMBOL (If applicable)	9 PROCUREMENT INSTRUMENT IDENTIFICATION NUMBER: F33615-81-C-2058
8c ADDRESS (City, State and ZIP Code)	10 SOURCE OF FUNDING NOS

PROGRAM ELEMENT NO	PROJECT NO	TASK NO	WORK UNIT NO
62203F	3145	19	10

11 TITLE (Include Security Classification): DLTS Analysis and Modeling of Electron and Proton Irradiated GaAs Multijunction Solar Cells

12. PERSONAL AUTHOR(S): Sheng S. Li

13a TYPE OF REPORT	13b TIME COVERED	14 DATE OF REPORT (Yr., Mo., Day)	15 PAGE COUNT
Final	FROM 10/85 TO 10/86	1987/Mar.	49

16 SUPPLEMENTARY NOTATION: This effort was accomplished under the AFWAL/POO Scholarly Research Program

17. COSATI CODES		
FIELD	GROUP	SUB GR
10	01	
22	02	

18 SUBJECT TERMS (Continue on reverse if necessary and identify by block number): DLTS, AlGaAs, GaAs, InGaAs, Germanium, Radiation Defects, Multijunction Solar Cells, DX Centers, Tunnel Junctions.

19 ABSTRACT (Continue on reverse if necessary and identify by block number)

A numerical model has been developed to calculate the displacement defects, the damage constant of minority-carrier diffusion length and the degradation of short-circuit current (I_{sc}), open-circuit voltage (V_{oc}) and conversion efficiency (η_c) in the 1-MeV electron- and proton-irradiated AlGaAs/GaAs/InGaAs multijunction junction solar cell under normal incidence conditions. The results show good agreement between our calculated values and the experimental data of I_{sc}, V_{oc} and η_c. In addition, DLTS analysis of defects in AlGaAs p-n junction solar cells irradiated by 1-MeV electrons has also been carried out in this work. The I-V analysis on several MOCVD-grown Ge/GaAs tunnel junction diodes has also been made in this study.

20 DISTRIBUTION/AVAILABILITY OF ABSTRACT	21 ABSTRACT SECURITY CLASSIFICATION	
UNCLASSIFIED/UNLIMITED ☒ SAME AS RPT ☐ DTIC USERS ☐	Unclassified	
22a NAME OF RESPONSIBLE INDIVIDUAL: Lt. Michael Chung	22b TELEPHONE NUMBER (Include Area Code): (513) 255-6235	22c OFFICE SYMBOL: AFWAL/POOC-2

DD FORM 1473, 83 APR — EDITION OF 1 JAN 73 IS OBSOLETE

Contents

1. Modelling of Radiation Damage Due to Electron and Proton Irradiation

1.1 Introduction

The purpose of this research project was to evaluate the performance of the proton- or electron-irradiated single junction and multijunction solar cells. This study was an extension of the work previously done under contract to WPAFB on theoretical calculations of displacement damage in the proton- or electron- irradiated AlGaAs/GaAs/InGaAs and AlGaAs/GaAs/Ge multijunction solar cells (contract No. F33615-81-2058).

In this report a modified theoretical model for computing the short-circuit current (I_{sc}) degradation in the proton- or electron- irradiated (AlGa)As-GaAs single junction solar cells is presented. In this model we assume that the radiation- induced displacement defects form an effective recombination center which controls the electron and hole lifetimes in the junction space charge region and in the n-GaAs active layer of the irradiated GaAs p-n junction cells. In order to determine the I_{sc} degradation, the displcement defect density D(E), path length P, range R, reduced energy after penetrating a distance x and the average number of displacement formed by one proton or electron scattering event were calculated first. The improvements of our modified model are threefold: (1) Instead of using equal capture cross sections for both electrons and holes it uses the electron- capture cross section in the p-diffused layer and the hole-capture cross section in the n-base layer. (2) It uses the wavelength- dependent absorption coefficients, not an average absorption coefficient. (3) It considers the reduced energy of incident electons or protons after penetrating through the window layer. As for the multijunction solar cells cases, this model is still valid and will be elaborated in section 1.2.

Excellent agreement is obtained between our calculated values and the measured I_{sc} in the proton or electron irradiated GaAs solar cells for proton energies ranging from 100 KeV to 10 MeV and fluences from 10^{10} *to* 10^{12} cm^{-2}, and electron energy of one MeV and fluences from 10^{14} *to* 10^{16} cm^{-2}. In addition, the damage constants of the minority-carrier diffusion lengths and degradations of the open-circuit voltage (V_{oc}) and conversion efficiency (η_c) for the single and multijunction solar cells such as GaAs, (AlGa)As/GaAs and (AlGa)As/GaAs/(InGa)As are also performed in this report.

1.2 Calculations of I_{sc} Degradation

1.2.1 Displacement Damage

A solid may be affected in two ways by the energetic particle bombardments as follows: [Reference 1] (1) Lattice atoms may be removed from their regular lattice sites, producing displacement damage, (2) the irradiating particle may cause change in the chemical properties of the solid via ion implantation or transmutation.

In the displacement model, it is assumed that the dominant defect produced by incident protons is due to lattice displacement. Under this assumption, an atom will be invariably displaced from its lattice site during collisions if its kinetic energy exceeds the threshold energy (T_d) for the atomic displacement to take place. Conversely the atom will not be displaced if its kinetic energy is less than T_d [Reference 2]. We assume that the transferred energy (T) to the struck atom is transformed only into the kinetic energy. If T is sufficiently large (i.e., $T \gg T_d$), then additional displacement can be produced by the recoiling nucleus before coming to rest at an interstitial site. Therefore, for $T > T_d$, the total number of displacement produced by a normal incident proton or electron to the solar cell can be calculated by using the expressions:

$$D(E_o) = \int_0^R N\sigma V\, dR \tag{1.1}$$

where $D(E_o)$ is the number of displacement per incident proton or electron, E_o is the initial energy of an incident proton or electron, N is the number of atoms per unit volume of the solar cell, σ is the displacement cross section for energetic protons or electrons, V is the average number of displacements formed by one proton- or electron- scattering event, and R is the range of proton or electron of energy E_o.

Since the mass of proton is heavy, it is necessary to consider the multiple scattering effect of the proton. Therefore, $D(E_o)$ with multiple scattering effect is obtained by replacing R with path length P in equation (1.1). However, the difference between the path length and the range for a proton traveled in coming to rest in a GaAs, (AlGa)As, (InGa)As or Ge solar cell is less than 5 % for those proton energies greater than 1 MeV. Thus, the multiple scattering effect is important only for low energetic protons. The empirical formulae for the path length, range and reduced energy (E_{re}) after penetrating a distance x are obtained by fitting the data of Janni [Reference

3] for protons and the data of Pages et al. [Reference 4] for electrons. It should be noted that a comprehensive study of the displacement damage in GaAs has been performed and reported in our previous contract technical report submitted to the AF Aeropropulsion Lab. last year.

1.2.2 Calculations of I_{sc} Degradation

For an (AlGa)As-GaAs single junction solar cell the total I_{sc} is equal to the sum of I_{sc} in the (AlGa)As window layer, in the p-GaAs layer and n-GaAs layer as well as in the depletion region of the junction. Since the spectral response of the window layer is much less than that of the whole solar cells [Reference 5] and the thickness of the window layer is less than 0.5 μm, it is reasonable to assume that the I_{sc} degradation of the window layer is negligible compared to the total I_{sc} degradation of the cell. It should be noted that the I_{sc} degradation mechanism for a two- or three-junction cell is similar to a single- junction cell, with the exception that we treat the first or the second cell as the window layer for the second or the third cell, respectively.

To derive an expression for the I_{sc} in a proton- or electron- irradiated GaAs p-n junction solar cell, the following assumptions are made : [References 6-9] (1) Radiation-induced defects do not alter the internal electric field, (2) radiation induced defects alter the cell performance mainly through changes of the minority carrier lifetimes in the bulk, and (3) radiation-induced displacements within the solar cell form recombination centers for the minority carriers of electron-hole pairs produced by photon absorption.

The short circuit current, I_{sco}, for the unirradiated solar cell is given by :

$$I_{sco}(\lambda) = \int_0^t \eta(x)p(x,\lambda)dx \tag{1.2}$$

and for the damaged cell, the I_{sc} can be expressed by [References 9-12]

$$I_{sc}(\lambda) = \int_0^t \eta(x)[1 - F(x)]p(x,\lambda)dx \tag{1.3}$$

The normalized I_{sc} degradation can thus be calculated by using the expression:

$$\frac{I_{sc}}{I_{sco}} = \frac{\int_{\lambda_1}^{\lambda_2} I_{sc}(\lambda)d\lambda}{\int_{\lambda_1}^{\lambda_2} I_{sco}(\lambda)d\lambda} \tag{1.4}$$

where

$$F(x) = 1 - E_2[\sqrt{6}\sigma_r\Phi|D(E_x) - D(E_{x_j})|]$$

is the recombination loss coefficient. $E_2(z)$ is the exponential integral of order 2. σ_r is the electron- or hole- capture cross section. Φ is the proton fluence. D(E) is the total number of displacement. E_x is the reduced proton energy after penetrating a distance, x. x_j is the junction depth. $p(x,\lambda) = K\alpha\exp(-\alpha x)$ is the photon generation rate at depth x. K is the integrated solar photon flux in the absorption band. α is the absorption coefficient. $\eta(x)$ is the current collection efficiency.

Note that t is the thickness of the cell and λ_1 and λ_2 denote the short-wave and long-wave limits of the total useful solar spectra for the GaAs cell (i.e. $\lambda_1 = 0.35$ μm and $\lambda_2 = 0.9$ μm).

1.3 Calculations of the Damage Constants

The damage coefficient of the minority carrier diffusion length is related to the proton or electron fluence by the relation:

$$\frac{1}{L^2} = \frac{1}{L_o^2} + K_L\Phi \tag{1.5}$$

where L is the minority-carrier diffusion length after proton- or electron- irradiation, L_o is the initial minority-carrier diffusion length. Φ is the proton- or electron- fluence. K_L is the damage constant of the minority-carrier diffusion length. Using $L^2 = D\tau$, Eq.(5) becomes

$$\frac{1}{\tau} = \frac{1}{\tau_o} + K_\tau\Phi \tag{1.6}$$

where τ is the minority-carrier lifetime after proton- or electron- irradiation; τ_o is the minority-carrier lifetime before proton- or electron- irradiation, and $K_\tau = DK_L$ is the damage constant of the minority-carrier lifetime. Expression for τ is given by :

$$\tau = \frac{1}{N_t V_{th}\sigma} \tag{1.7}$$

where V_{th} is the thermal velocity; σ is the capture cross section of the trap, and N_t is the total trap density. The trap density N_t can be estimated directly from the total number of displacement defect density D(E) per unit penetration depth whose value is calculated as a function of incident proton energy by using the displacement damage theory.

1.4 Degradations of V_{oc} and η_c

In general, the open-circuit voltage of a solar cell can be represented by the following equation:

$$V_{oc} = (\frac{nkT}{q}) \ln(\frac{I_{sc}}{I_o} + 1) \tag{1.8}$$

where n is the diode ideality factor and I_o is the saturation current. In using Eq.(1.8), it is assumed that I_o is dominated by the diffusion component. In this case the saturation current is given by

$$I_o = (qn_i^2 A)(\frac{D_p}{L_{po} N_D} + \frac{D_n}{L_{no} N_A}) \tag{1.9}$$

where n_i is the intrinsic carrier density, A is the area of the solar cell, D_p is the hole diffusion coefficient, D_n is the electron diffusion coefficient, L_{po} is the hole diffusion length, L_{no} is the electron diffusion length, N_D is the donor dopant density, and N_A is the acceptor dopant density.

Now combining Eq.(1.9) and Eq.(1.5), the saturation current after the proton or electron irradiation is given by

$$I_o' = (qn_i^2 A)(\frac{D_p}{L_p N_D} + \frac{D_n}{L_n N_A}) \tag{1.10}$$

where

$$\begin{aligned} L_p &= (K_{Lp}\Phi + \frac{1}{L_{po}^2})^{-1/2} \\ L_n &= (K_{Ln}\Phi + \frac{1}{L_{no}^2})^{-1/2} \end{aligned} \tag{1.11}$$

K_{Lp} is the damage constant of the hole diffusion length and K_{Ln} is the damage constant of the electron diffusion length.

Now substituting Eqs.(1.9) and (1.10) into Eq. (1.8) yields the degradation of the open circuit voltage as follows

$$\frac{V_{oc}}{V_{oco}} = \frac{\ln(I_{sc}/I_o' + 1)}{\ln(I_{sco}/I_o + 1)} \tag{1.12}$$

Since the dark current of GaAs solar cells tend to be dominated by the recombination current (I_{rg}) at low voltage (< 0.8 V) and dominated by the injection current at higher voltage [Reference 13], therefore, for V_{oc} less than 0.8 V, V_{oc} becomes

$$V_{oc} = (\frac{nkT}{q}) \ln(\frac{I_{sc}}{I_{rg}}) \tag{1.13}$$

where the ideality factor n is two and I_{rg} is given by

$$I_{rg} = \frac{(qn_iW)}{(\tau_p\tau_n)^{1/2}} \tag{1.14}$$

where W is the depletion width, and τ_p and τ_n are the hole and electron lifetimes in the n- and p-region, respectively. However, for the (AlGa)As cell the dark current is assumed to be recombination- dominant because the ideality factor of the (AlGa)As cell is greater than 2.0.

The maximum power (P_{max}) of a solar cell can be represented by the product of I_{sc}, V_{oc} and the fill factor F.F.. If there is no significant change in fill factor after the proton- or electron-irradiation in (AlGa)As-GaAs solar cells, then the degradation of the conversion efficiency can be expressed by

$$\frac{\eta_c}{\eta_{co}} \simeq \frac{I_{sc}V_{oc}}{I_{sco}V_{oco}} \tag{1.15}$$

1.5 Results and Discussion

Fig. 1.1 [1] shows the physical structure and dimensions of an (AlGa)As-GaAs single- junction solar cell used in our study. The wide bandgap Be-doped $Al_{0.85}Ga_{0.15}As$ epilayer was grown by infinite solution liquid-phase epitaxy (LPE) with dopant density of $3-5\times10^{18}$ cm^{-3} and used as a window layer to reduce the surface recombination at the p-GaAs surface. A thin window layer of less than 0.5- μm thick and a diffused junction depth of less than 0.5 μm were used to ensure the low optical absorption loss and to increase the radiation hardness [Reference 14].

Fig. 1.2 shows the I_{sc} degradation in the proton- irradiated $Al_{0.85}Ga_{0.15}As$ - GaAs single- junction solar cell. The solid curves are from our calculations, and the solid dots are from experimental data. As shown in Fig. 1.2 the maximum I_{sc} degradation was created by the 200 KeV protons. The reason for the 200 KeV protons create much more damage than those higher energy protons is that most of the damages caused by 200 KeV protons occurred in the junction and inside the active region of the n-GaAs layer.

The parameters involved in the I_{sc} degradation calculations are absorption coefficients of cells, current collection efficiency, electron- and hole- capture cross sections, total number of displacement defects formed as well as fluences and energy of protons. In order to calculate the total number of

[1] Figures and tables are located at the back of this report (pages 21 through 39)

displacement defects, parameters such as P, R and E_{re} of incident protons should be also calculated. In our computer simulation, we have assumed that the absorption coefficients and current collection efficiency of the solar cell remain constant after irradiation. According to Eq. (1.3), since the fluence of protons through the entire solar cells is constant and the total number of displacement defects are bound to the initial energy of incident protons, the values selected for electron- and hole- capture cross sections are critical to the accuracy of I_{sc} degradation calculations. The values of parameters used in our simulation are listed in Table 1.1.

Since the I_{sc} degradation in the (AlGa)As window layer is negligible, it is reasonable to calculate the I_{sc} degradation only in the GaAs solar cell. In our simulation we first calculated E_{re} after penetrating the window layer. If E_{re} is equal to zero, then there is no damage to the GaAs solar cell. Otherwise, E_{re} would be applied as the initial energy of the proton for the GaAs solar cell. According to our calculation, the proton would lose 50 KeV energy after penetrating through a 0.34- μm thick window layer. Therefore, no damage to the GaAs solar cell would result if the incident proton energy is less than 50 KeV.

It is appropriate to use two different recombination cross sections (i. e., σ_n in the p-region, and σ_p in the n-region of the solar cell) for our computer simulation since the recombination mechanism is controlled by the electron- capture cross section in the p-region and by the hole- capture cross section in the n-region. We have used the best value of 1.8×10^{-14} cm^2 for electron- capture cross section in the p-region and 1.5×10^{-13} cm^2 for hole- capture cross section in the n-region in our calculations. These values are based on the results obtained from DLTS measurements [Reference 8], and are consistent with the fact that the radiation-hardness of the p-type GaAs is greater than that of the n-type GaAs.

Table 1.2 through Table 1.4 are values of input parameters and I_{sc} degradations of the proton irradiated $Al_{0.85}Ga_{0.15}As$ - $Al_{0.40}Ga_{0.60}As$ single- junction solar cell and $Al_{0.40}Ga_{0.60}As$-GaAs two-junction solar cells. They show that the radiation-hardness of an (AlGa)As solar cell is greater than that of a GaAs cell. This is reasonable because the electron- and hole- capture cross sections of the (AlGa)As cell are less than those of the GaAs cell. Table 1.5 is the I_{sc} degradation for the proton-irradiated $Al_{0.35}Ga_{0.65}As/GaAs/In_{0.53}Ga_{0.47}As$ triple- junction solar cell.

The damage constants of the minority carrier diffusion lengths for the GaAs, $Al_{0.35}Ga_{0.65}As$ single- junction solar cell and $Al_{0.35}Ga_{0.65}As/GaAs/In_{0.53}Ga_{0.47}As$ triple- junction solar cells are

summarized in Table 1.6 through table 1.8. The results show that for proton energies greater than 0.3 MeV, the damage constant of the electron- or hole- diffusion length decreases as the proton energies increased. This is consistent with our previous calculations on I_{sc} degradations in these cells.

Table 1.9 shows the degradations of I_{sc}, V_{oc} and η_c obtained from our theoretical calculations and experimental data in the proton irradiated $Al_{0.85}Ga_{0.15}As$-GaAs single junction solar cell. It is found that our calculated degradations are in good agreement with the experimental data for proton energies on 0.1, 0.3, 1, 2, 5 and 10 MeV and fluences from 10^{10} to 10^{12} cm^{-2}.

Table 1.10 through table 1.11 are the values of input parameters for calculating the degradation of I_{sc}, V_{oc}, η_c and damage constants of the minority carrier diffusion lengths and those calculated results in a 1- MeV electron-irradiated (AlGa)As-$Al_{0.33}Ga_{0.67}As$ single junction solar cell. The results are in good agreement with the expermental data for electron fluences of 10^{14} and 10^{15} cm^{-2}. Values of the input parameters and the I_{sc} degradation of the 1- MeV electron irradiated $Al_{0.40}Ga_{0.60}As$-GaAs two- junction solar cells are shown in Table 1.12 and Table 1.13, respectively. It is found that the degradation decreases when the thickness of the top cell decreases.

1.6 Conclusion

A rigorous model for computing the degradations of I_{sc}, V_{oc}, η_c and the damage constants of the minority carrier diffusion lengths in the proton- or electron- irradiated GaAs, (AlGa)As/GaAs and (AlGa)As/GaAs/(InGa)As solar cells has been developed in this work. The results show that excellent agreement between our calculated values and the experimental data of the degradations of I_{sc}, V_{oc} and η_c was obtained in the proton- irradiated $Al_{0.85}Ga_{0.15}As$-GaAs single- junction solar cell and in the electron- irradiated $Al_{0.85}Ga_{0.15}As$ - $Al_{0.33}Ga_{0.67}As$ single- junction solar cell.

2. DLTS Analysis of Defects in Electron- Irradiated AlGaAs and Ge-GaAs Diodes

2.1 Introduction

The objective of this research is to investigate the radiation-induced deep-level defects in the 1-MeV electron irradiated $Al_xGa_{1-x}As$ ($0.3 < x < 0.33$) using the Deep Level Transient Spectroscopy (DLTS), Capacitance-Voltage (C-V) and Current-Voltage (I-V) techniques. 1-MeV electron or low energy proton is usually used in order to simulate the space environment. The defect parameters such as the activation energy, defect density and capture cross section deduced from the DLTS and C-V measurements, gives the comparative informations for the unirradiated and irradiated solar cells. The latter informations help us design a radiation- hard cascade solar cell using materials such as GaAs, $Al_xGa_{1-x}As$ and germanium.

The results obtained from this study will be described next. The method of determining the exact densities of two DX centers under the condition of total carrier freeze-out at liquid nitrogen temperature, in which the apparent values of DX centers determined by the DLTS measurement are far below the actual ones, has been developed by using the combined TSCAP (i.e., Thermally-Stimulated CAPacitance method) and constant- temperature C-V methods. The DLTS characterization on the unirradiated Te-doped $Al_{.3}Ga_{.7}As$ and 1-MeV electron irradiated $Al_xGa_{1-x}As$ are described, and the conclusion is included in this report.

2.2 An Accurate Determination of DX-Center Density in Sn-doped $Al_xGa_{1-x}As$

It is well- known that the dominant deep-electron traps, known as the DX- centers play a major role in controlling the electrical characteristics of this alloy system for $x > 0.2$. It has been reported recently that no ionized donors are observable below 150 K in the MBE- grown Si-doped $Al_{.35}Ga_{.65}As$ [Reference 15]. A significant decrease of the free carrier concentration and Hall mobility as well as a marked carrier freeze-out are observed if the Al content is increased beyond $x = 0.25$ [Reference 16,17]. The overall concentration of deep electron traps is greatly enhanced near the direct-to-indirect bandgap crossover point [Reference 18]. For alloy composition with $x = 0.35 \pm 0.02$, the DX centers govern the electrical properties of the $Al_xGa_{1-x}As$ [Reference 19]. The DX center is a substitutional deep-donor state with its activation energy associated with the L- conduction band

minima [Reference 20,21]. For $x > 0.3$, the density of DX center can be exceed the background density, and hence accurate determination of DX center density becomes extremely difficult for x greater than 0.30.

In this study, an accurate method of determining the density of DX centers and other deep electron traps in the LPE- grown Sn-doped $Al_xGa_{1-x}As$ epilayer (with $0.2 < x < 0.4$) using a combined DLTS, TSCAP, and constant temperature C-V techniques is presented. It will be shown that from the study of two dominant electron traps observed in the Sn-doped $Al_xGa_{1-x}As$ one can obtain the information concerning the role of DX centers and their relationship to the free carrier density in the conduction band of $Al_xGa_{1-x}As$ if the DX centers are assumed as native defects associated with the multivalley conduction band structures. The DLTS spectra for four Sn-doped $Al_xGa_{1-x}As$ samples with $x = 0.2$, 0.3, 0.33, *and* 0.40 are shown in Fig.2.1. The Sn-doped $Al_xGa_{1-x}As$ samples always exhibit two dominant DX centers with energies of $E_c - 0.20$, and 0.30 eV. As the aluminum mole fraction ratio increases, the concentration of DX centers also increase dramatically, particularly for $x > 0.3$. Our low-temperature C-V measurements revealed that a complete carrier freeze-out occured at 77 K for $Al_{.33}Ga_{.66}As$ As and $Al_{.4}Ga_{.6}As$ samples. The results clearly show that the shallow donor concentration is smaller than the density of the dominant DX centers. Therefore, the free electron density in the conduction band measured at 300 K is mainly contributed by the DX centers. This new result supports the recently proposed model that the DX centers are the substitutional donors in AlGaAs alloy system [Reference 20].

In the case in which the concentration of DX centers is very large, the simple relation that $N_T = 2[\triangle C(0)/C]N_D$ used in the conventional DLTS analysis is no longer valid. In the cases of $Al_{.33}Ga_{.67}As$ and $Al_{.4}xGa_{.6}As$ samples, determination of the exact density of DX- centers was impossible by using the DLTS technique due to the carrier freeze-out at low temperature. Therefore, for $x > 0.33$, the DLTS measurements may introduce a large error in determining the density of the DX centers. The apparent density measured by the conventional DLTS analysis would be much smaller than the actual density since most free carriers are supplied by the DX centers themselves. Another interesting phenomena observed in the $Al_{.33}Ga_{.66}As$ sample was that in the DLTS thermal scan a small positive DLTS peak appeared, which was caused by the capture of electrons by the unfilled DX centers at low temperatures [Reference 22]. When a small forward-biased pulse was applied, the positive peak disappeared. This means that by applying a saturation pulse a sufficiently large electron density is supplied to the p-n junction, and the DX centers will be filled by electrons

during the injection pulse (30 ms) at low temperature. This procedure can be used to eliminate the electron- capture by the unoccupied DX centers. To provide an accurate determination of the density of DX centers, the density of DX centers was determined by the TSCAP measurements for both $Al_{.33}Ga_{.67}As$ and $Al_{.4}Ga_{.6}As$ samples, using the equation given by [Reference 23,24]

$$C_2^2 - C_1^2 = \left[\frac{A^2 q \epsilon_o \epsilon_s}{2(V_D + V_R)}]N_T\right] \tag{2.1}$$

where C_1 and C_2 are the values of capacitance taking from the capacitance step observed in the TSCAP scan, as is shown in Fig.2.2. For large trap density, the relation, $N_T = 2[\Delta C(0)/C]N_D$ was no longer valid, and Eq.(2.1) should be used intead. The TSCAP curve clearly shows two capacitance steps for the $Al_{0.33}Ga_{0.67}As$ sample, and the locations of capacitance steps coincide well with those DLTS peaks for the DX centers shown in Fig.2.1. However, for the $Al_{.4}Ga_{.6}As$ sample, there are two closely spaced capacitance steps. Comparing the spectrum of TSCAP scan for the $Al_{.4}Ga_{.6}As$ sample with that of DLTS scan, it is clear that the density of $E_c - 0.20$ eV level is higher than that of the $E_c - 0.30$ eV level. A typical constant- temperature C-V measurement for the $Al_{.4}Ga_{.6}As$ sample is shown in Fig.2.3. The result shows a complete carrier freeze-out at 77 K for both $Al_{.33}Ga_{.67}As$ and $Al_{.4}Ga_{.6}As$ samples, whereas no carrier freeze-out was observed for $Al_{.2}Ga_{.8}As$ and $Al_{.3}Ga_{.7}As$ samples. This result clearly illustrates that the free carriers at room temperature are supplied mostly by the DX centers for $x > 0.33$. This result is consistent with the x- composition- dependent electron mobility in which the Hall mobility decreases abruptly for $x > 0.3$. For alloy compositions in the range $0 < x < 0.3$, the electron mobilities are reduced due to the increasing contribution from the alloy scattering, and no intervalley scattering is required to explain the data [Reference 25]. In addition, the mobility due to alloy scattering has been found to be approximately an order of magnitude larger than that of the space- charge scattering for $Al_xGa_{1-x}As$ ($x < 0.32$) [Reference 26]. For alloy compositions in the range $0.32 < x < 0.6$, intervalley scattering among the various minima is required to explain the data [Reference 27,28]. For low ($0 < x < 0.3$) and high ($0.5 < x < 1.0$) composition range, the calculated drift mobility can be directly compared with the Hall mobility. This is, however, invalid for the intermediate composition range ($0.3 < x < 0.5$) due to the multi- conduction band transport [Reference 25]. The difficulty arises from the fact that various material parameters are not well established in this alloy composition range.

It is noted that for the Te- or Se-doped $Al_xGa_{1-x}As$ samples there are two DX centers peaks in the $0.3 < x < 0.6$ range while only one peak exists for the $0.2 < x < 0.3$ or $0.6 < x < 1.0$

range [Reference 22]. This result suggests that the two DX centers are possibly associated with the L and X conduction bands, respectively in the $0.3 < x < 0.5$ composition range. Based on this result, it is obvious that an accurate determination of the density of the two DX centers in Sn, Se or Te-doped samples in the $0.3 < x < 0.5$ range can give the much needed information for understanding the relative importance of Γ, L, and X conduction bands and the interpretation of transport properties in this composition range. Another complication associated with the DX centers in the $Al_xGa_{1-x}As$ system is that different species of donor impurities give rise to slightly different energy states in the forbidden energy gap such as activation energy, one or two DX centers. Therefore, additional theoretical and experimental studies are definitely needed for the $Al_xGa_{1-x}As$ system in the composition range $0.3 < x < 0.5$ in order to obtain a better understanding concerning the electrical and transport properties in this material. The results of DLTS, TSCAP and C-V measurements on the LPE- grown $Al_xGa_{1-x}As$ samples are summarized in Table.2.1.

In short, electrical characterization of Sn-doped $Al_xGa_{1-x}As$ ($0.2 < x < 0.4$) grown by the LPE technique has been carried out using the combined DLTS, constant- temperature C-V and TSCAP measurements. The total carrier freeze-out was observed for $x > 0.33$ at 77 K, in which the electron mobility also shows a sharp decrease. The combined DLTS, TSCAP, and C-V measurements enable an accurate determination of the density of DX centers in $Al_xGa_{1-x}As$ for $x > 0.3$.

2.3 DLTS Analysis of the LPE-Grown Te-Doped $Al_{.3}Ga_{.7}As$

The Te-doped $Al_{.3}Ga_{.7}As$ was investigated by using the DLTS, constant temperature C-V, and TSCAP measurements. The results are summarized as follows: One electron trap with energy of E_c - 0.33 eV (DX center) was observed in this sample. The measured capture cross section is $2.42 \times 10^{-13}\ cm^2$. Net doping density N_D at 300 K is $2 \times 10^{17}\ cm^{-3}$, and $2.03 \times 10^{16}\ cm^{-3}$ at 77 K, as determined by the constant- temperature C-V measurement. The unusual high concentration of tellurium impurity found in this LPE- grown AlGaAs sample is closely related to the high concentration of the DX center detected by the DLTS measurement. The defect density of DX center determined by both the TSCAP and DLTS measurements was found to be nearly the same, namely, $1.90 \times 10^{17}\ cm^{-3}$ and $1.79 \times 10^{17}\ cm^{-3}$, respectively. The equations for computing the

trap density are given by

$$C_2^2 - C_1^2 = \left[\frac{A^2 q \epsilon_o \epsilon_s}{2(V_D + V_R)}\right] N_T \qquad for\ TSCAP \tag{2.2}$$

$$N_t = \left[\frac{\Delta C(2C_o - \Delta C)}{C_o^2}\right] N_D \qquad for\ DLTS \tag{2.3}$$

The measured value of ΔC was determined at the temperature where the DLTS peak occured when the temperature was stabilized. Accordingly, the estimated ΔC and hence the value of N_t from the TSCAP measurement using Eq.(1), is very accurate.

2.4 DLTS Analysis of the 1- MeV Electron- Irradiated $Al_xGa_{1-x}As$

The DLTS, I-V and C-V measurements were performed on the Te-doped $Al_xGa_{1-x}As$ ($0.3 < x < 0.33$) p-n junction cells irradiated by the 1- MeV electrons with fluences of 10^{14} and 10^{15} cm^{-2}. Defect parameters determined from these measurements are summarized in Table 2.3. The DLTS measurements showed that two electron traps (DX centers) were dominant in these irradiated cells as is shown in Fig. 2.4. The physical origin of these DX centers are closely related to the shallow dopant, and their densities are exactly proportional to the room temperature free- carrier density. For the 1-MeV electron irradiated samples, additional trap levels (i.e., one electron trap and one hole trap) with very small trap density ($N_t/N_D = 0.002$) were observed in the high-temperature regime. However, the activation energies and capture cross sections were not able to determine because their transient signals were too weak to be drawn on the DLTS spectra. These transient signals began to appear around 200 K and continued to show up above 450 K which were the maximum raisable temperature limit of our system. When we compare this results with the neutron-irradiated ones, a common phenomenon of long tail of DLTS signal could be observed. As for the neutron- irradiated $Al_xGa_{1-x}As$, there have been reported for the deep-level of a long tail, which is ascribed to defect clusters [Reference 29]. The electron irradiation, however, cannot transfer enough energy into the knock-on atoms to form the high density of defect cluster. The 1-MeV electron irradiation might just cause trace of similar type of defect cluster but of very small density compared with the neutron-irradiation. These traps were of very small densities, but they were deep enough to stand for the small degradation of $Al_xGa_{1-x}As$ solar cells irradiated by the 1-MeV electron with the fluence of 10^{15} cm^{-2}. Except for this fact, there were very small variations in the I-V and C-V characteristics with variation of the electron fluences. The ideality factor n

in the I-V characteristics showed the little variations of 2.06, 2.14 and 2.17,with the fluences of 0, 10^{14} *and* 10^{15} cm^{-2}, respectively, as are shown in Fig. 2.5. The C-V curves shown in Fig. 2.6 are nearly identical, indicating the very small carrier removal rate with the 1- MeV electron-irradiation.

In short, the 1- MeV electron- irradiation introduces a small damage in the Te-doped $Al_xGa_{1-x}As$ solar cells ($0.3 < x < 0.33$).

2.5 I-V Characteristics of the MOCVD-Grown Germanium and Ge-GaAs Diodes

The I-V measurements were performed on samples OM-506 (n^+ - Ge: p-Ge), OM-507 (p^+ - Ge: n-Ge), OM-514(A) (p^+ - Ge: p^+ -GaAs), and OM-514 (B) (p^+ - Ge: n^+ - GaAs). The results showed that all these samples had either ohmic behavior or very low barrier. The results for samples OM-506 and OM-507 showed nonideal ohmic characteristics. These germanium homojunction diodes (OM-506 and OM-507) yielded back-to-back diode I-V characteristics. It is likely that the large density of copper impurity in these diodes might account for this anomalous behavior.

The Ge-GaAs heterojunction diodes (OM-514 (A) and OM-514 (B)) showed clearly the ohmic behavior. It is obvious that the observed I-V characteristics for these diodes is contributed by both the thermionic emission current and the tunneling current through the heterojunction. Thermionic emission current is expected to be dominated at room temperature while tunneling current becomes significant at low temperature. It has been shown that all heterojunction diodes fabricated with n_{GaAs} with dopant densities greater than 8×10^{16} cm^{-3} are ohmic at 300 K and at 77 K [Reference 30].

The I-V characteristics for heterojunction can be fitted by using the empirical equation [Reference 30]

$$J = aV \exp(-E/kT) \tag{2.4}$$

where a is independent of T.

For the Ge-GaAs heterojunction of doping range, $n_{Ge} = 10^{18}$ cm^{-3} and $n_{GaAs} = 5 \times 10^{15}$ cm^{-3}, the fitted value of E is reported as 80 ± 10 meV. The measured values of E are 3.56 and 5.53 meV, respectively for the OM-514 (A) and OM-514 (B), respectively. Increasing background-

dopant density decreases the value of E significantly. The voltage- dependence of the current is a manifestation of the barrier lowering effect with voltage. The lowering of the heterojunction barrier with increasing voltage is similar to that of the metal- semiconductor barrier [Reference 31]. The specific contact- resistance defined by $R_c = dI/dV$ *at* $V = 0$ derived for each diode is shown in table 2.4.

2.6 Conclusion

An accurate determination of the density of DX-centers in $Al_xGa_{1-x}As$ materials in the range of $x > 0.30$, in which a total carrier freeze-out at 77 K occured, has been made by using the combined TSCAP and constant- temperature C-V methods. The Sn-doped $Al_xGa_{1-x}As$ ($0.2 < x < 1$) shows two DX-center peaks, whereas the Te-, Se-, and Si-doped AlGaAs samples show two DX-center peaks in the range of $0.3 < x < 0.5$, which have not been reported in the literature. The method presented here is a very useful tool for the determination of defect parameters in the range of $x > 0.3$.

In the 1-MeV electron- irradiated Te-doped $Al_xGa_{1-x}As$ ($0.3 < x < 0.33$), no significant irradiation- induced defects were found in these samples.

The I-V measurements on the n^+-Ge/p-Ge, p^+ - Ge/n-Ge, p^+ - Ge/p^+ - GaAs and p^+/n - GaAs junction diodes have been performed in this study. The germanium homojunction diodes yield back-to-back diode I-V characteristics. It is likely that the large density of copper impurity found in these diodes might account for this anomalous behaviour. The Ge/GaAs heterojunction diodes have shown good ohmic behaviour which is a result of the barrier lowering due to the increased background- doping density in these diodes. The Ge/GaAs tunnel junction diodes may be used for the cascade solar cell application.

References

[1] N. L. Peterson and S. D. Harkness, eds., *Radiation Damage in Metals*, American Soc. for Metals, C, pp.59, 1976.

[2] G. J. Dienes and G. H. Vineyard, *Radiation Effects in Solids*, Interscience Publishers Inc., New York, 1957.

[3] J. F. Janni, *Proton Range-Energy Tables, 1 Kev- 10 GeV*, Atomic Data and Nuclear Data

Tables 27, pp.147, 1982.

[4] L. Pages, E. Bertel, H. Joffre and L. Sklavenitis, *Energy Loss, Range and Bremsstrahling Yield for 10 KeV to 100 MeV Electron in Various Elements and Chemical Compounds,* Atomic Data, Vol. 4, pp. 1-127, 1972.

[5] R. C. Knechtli, R. Y. Loo and G. S. Kamath, *High-Efficiency GaAs Solar Cells, IEEE Trans. on Electron Devices,* Vol. ED-31, No. 5, pp. 577, 1984.

[6] G. H. Walker and E. J. Conway, *Short Circuit Current Changes in Electron Irradiated Al-GaAs/GaAs Solar Cells,* 13th IEEE Photovoltaic Specialist Conference, pp. 575, 1978.

[7] G. H. Walker and E. J. Conway, *Recovery of Shadow Junction GaAs Solar Cells Damaged by Electron Irradiation,* J. Electrochem. Soc. pp. 1726, 1978.

[8] S. S. Li, *Electronic Properties of Deep-Level Defects in Proton Irradiated AlGaAs-GaAs Solar Cells,* NASA Final Report, September 1981.

[9] J. W. Wilson, J. J. Stith and L. V. Stock, *A Simple Model of Space Radiation Damagein GaAs Solar Cell,* NASA Technical Paper 2242, 1983.

[10] J. W. Wilson, G. H. Walker and R. A. Outlaw, *Proton Damage in GaAs Solar Cells,* IEEE Trans. on Electron Devices, Vol. ED-31, NO. 4, pp. 421, 1984.

[11] J. W. Wilson and L. V. Stock, *Equivalent Electron Fluence for Space Qualification of Shallow Junction Heteroface GaAs Solar Cells*, IEEE Trans. on Electron Devices, Vol. ED-31, NO. 5, pp. 622, 1984.

[12] J. Y. Yaung, *Model of Solar Cell Proton Damage,* NASA Space Photovoltaic Research and Technology Conference, pp. 56, 1983.

[13] H. J. Hovel,*Solar cells,* in Semiconductors and Semimetals, Vol. II, 1975.

[14] R. Y. Loo and G. S. Kamath, *Radiation Damage in GaAs Solar Cells*, 14th IEEE Photovoltaic Specialist Conference, pp. 1090, 1980.

[15] N. S. Caswell, P. M. Mooney, S. L. Wright and P. M. Solomon, Appl. Phys. Lett. 48 (16), pp. 1093, 1986.

[16] T. Ishibashi, T. Tarucha, and H. Okamoto, Jpn J. Appl. Phys. 21, pp. l476, 1982.

[17] H. Kunzel, H. Jung, E. Schubert, and K. Ploog, J. Physique 43, Colloque C5, C5-175, 1982.

[18] K. Hikosaka, T. Mimura, and S. Hiyamizu, Inst. Phys. Conf. Ser. 63, pp. 233, 1982.

[19] H. Kunzel, K. Ploog, K. Wunstel, and B. L. Zhou, J. Electronic Materials, vol. 13, no. 2, pp. 281, 1984.

[20] M. Mizuta, M. Tachikawa, H. Kukimoto and S. Minomura, Jpn J. Appl. Phys. vol. 24, pp. l143, 1985.

[21] P. K. Bhattacharya, A. Majerfeld, and A. K. Saxena, Inst. Phys. Conf. Ser. no. 45, pp. 199, 1979.

[22] D. V. Lang, and R. A. Logan, Phys. Rev. B, vol. 19, no. 2, pp. 1015, 1979.

[23] C. T. Sah, L. L. Rosier and L. Forbes, Appl. Phys. Lett., vol. 15, no. 6, pp. 161, 1969.

[24] C. T. Sah et al., Solid State Electronics, vol. 13, pp. 759, 1970.

[25] A. K. Saxena and A. R. Adams, J. Appl. Phys., vol. 58, no. 7, pp. 2640, 1985.

[26] K. Kaneko, M. Ayale, and N. Watanabe, Proceedings of the Sixth International Symposium on GaAs and Related Compounds, Edinburg Conference, edited by C. Hillsum (Institutu of Physics, London, 1977).

[27] A. Saxena, J. Appl. Phys., vol. 52, no. 9, pp. 5643, 1981.

[28] A. Saxena, J. Electronic Materials, vol. 11, no.3, pp. 453, 1982.

[29] C. E. Barnes, T. E. Zipperian and L. R. Dawson, Journal of Electronic Materials, vol. 14, no. 2, pp. 95, 1985.

[30] J. M. Ballingal et al., J. Vac. Sci. Technol. B1(3), pp. 675, 1983.

[31] V. L. Rideout and C. R. Crowell, Solid State Electron. vol. 13, pp. 993, 1970.

Appendix

1. Empirical Formulae for Path length and Range

(i) $Al_{0.85}Ga_{0.15}As$ window layer :

For proton :

$$P = \begin{cases} 3.300891\ E^{0.550212} & E \leq 0.15\ \text{MeV} \\ 10.79623\ E^{1.163227} & E \leq 1.25\ \text{MeV} \\ 9.963561\ E^{1.565366} & E \leq 10.0\ \text{MeV} \end{cases}$$

$$R = \begin{cases} 5.010253\ E^{0.865712} & E \leq 0.175\ \text{MeV} \\ 10.31089\ E^{1.257302} & E \leq 1.500\ \text{MeV} \\ 9.561796\ E^{1.579760} & E \leq 10.00\ \text{MeV} \end{cases}$$

where P and R are in um and E is in MeV. Unless specify otherwise, the unit of length is in um and that of energy is in MeV.

For Electrons:

$$R = \begin{cases} -0.895767 + 101.9048xE + 3649.2866xE^2 - 5155.75xE^3 & E \leq 0.2\ \text{MeV} \\ -50.2875 + 727.3489xE + 819.0796xE^2 - 350.477xE^3 & E \leq 1.0\ \text{MeV} \\ -260.305 + 1446.344xE - 39.7561xE^2 + 0.82831xE^3 & E \leq 10\ \text{MeV} \end{cases}$$

(ii) $Al_{0.40}Ga_{0.60}As$ Solar Cell:

For proton :

$$P = \begin{cases} 3.541585\ E^{0.547829} & E \leq 0.15\ \text{MeV} \\ 11.76566\ E^{1.146997} & E \leq 1.25\ \text{MeV} \\ 10.30205\ E^{1.556580} & E \leq 10.0\ \text{MeV} \end{cases}$$

$$R = \begin{cases} 5.37874\ E^{0.873210} & E \leq 0.175\ \text{MeV} \\ 10.63238\ E^{1.247584} & E \leq 1.500\ \text{MeV} \\ 9.856092\ E^{1.572202} & E \leq 10.00\ \text{MeV} \end{cases}$$

For Electrons:

$$R = \begin{cases} -0.913188 + 104.1110xE + 3694.2997xE^2 - 5227.10xE^3 & E \leq 0.2 \text{ MeV} \\ -50.5646 + 734.9293xE + 830.7752xE^2 - 356.379xE^3 & E \leq 1.0 \text{ MeV} \\ -262.765 + 1463.058xE - 40.9225xE^2 + 0.85276xE^3 & E \leq 10 \text{ MeV} \end{cases}$$

(iii) $Al_{0.33}Ga_{0.67}As$ Solar Cell :

For Electrons:

$$R = \begin{cases} -0.905805 + 103.2968xE + 3661.0080xE^2 - 5180.95xE^3 & E \leq 0.2 \text{ MeV} \\ -50.0565 + 728.0881xE + 823.5880xE^2 - 353.384xE^3 & E \leq 1.0 \text{ MeV} \\ -260.369 + 1449.811xE - 40.6388xE^2 + 0.84676xE^3 & E \leq 10 \text{ MeV} \end{cases}$$

2. Empirical Formulae for Reduced Energy

(i) $Al_{0.85}Ga_{0.15}As$ window layer:

For proton :

Multiple Scattering:

$$E_{re} = \begin{cases} 0.125206\ E^{1.875158} & E \leq 0.07 \text{ MeV} \\ 0.102326\ E^{1.205425} & E \leq 0.275 \text{ MeV} \\ 0.142437\ E^{0.812657} & E \leq 1.25 \text{ MeV} \\ 0.230867\ E^{0.638220} & E \leq 10.0 \text{ MeV} \end{cases}$$

Without Multiple Scattering

$$E_{re} = \begin{cases} 0.159627\ E^{1.164662} & E \leq 0.10 \text{ MeV} \\ 0.143353\ E^{0.892092} & E \leq 0.45 \text{ MeV} \\ 0.179735\ E^{0.722203} & E \leq 2.00 \text{ MeV} \\ 0.256094\ E^{0.619708} & E \leq 10.0 \text{ MeV} \end{cases}$$

For Electrons:

$$E_{re} = \begin{cases} 0.006729 + 56.63820xE - 25964.783xE^2 + 6447600xE^3 & E \leq 0.06 \text{ MeV} \\ 0.024392 + 22.7070\ xE - 1153.987xE^2 + 37320.9xE^3 & E \leq 0.2 \text{ MeV} \\ 0.07436 + 10.7862\ xE - 50.4696xE^2 + 255.656xE^3 & E \leq 0.75 \text{ MeV} \\ 0.18051 + 6.96689\ xE + 1.39212xE^2 + 0.30856xE^3 & E \leq 10.0 \text{ MeV} \end{cases}$$

where E_{re} is in MeV; E_o is the initial energy in MeV, x is the distance in um.

(ii) $Al_{0.40}Ga_{0.60}As$ Solar CelL:

For proton :

Multiple Scattering:

$$E_{re} = \begin{cases} 0.108043\ E^{1.879974} & E \leq 0.07 \text{ MeV} \\ 0.093611\ E^{1.230323} & E \leq 0.275 \text{ MeV} \\ 0.135203\ E^{0.822349} & E \leq 1.25 \text{ MeV} \\ 0.219692\ E^{0.647184} & E \leq 10.0 \text{ MeV} \end{cases}$$

Without Multiple Scattering

$$E_{re} = \begin{cases} 0.148897\ E^{1.153296} & E \leq 0.10 \text{ MeV} \\ 0.137115\ E^{0.900279} & E \leq 0.45 \text{ MeV} \\ 0.173908\ E^{0.726625} & E \leq 2.00 \text{ MeV} \\ 0.242293\ E^{0.630012} & E \leq 10.0 \text{ MeV} \end{cases}$$

(iii) $Al_{0.33}Ga_{0.67}As$ Solar Cell:

For Electrons:

$$E_{re} = \begin{cases} 0.006717 + 56.21560xE - 25553.562xE^2 + 6300951xE^3 & E \leq 0.06 \text{ MeV} \\ 0.024340 + 22.5947\ xE - 1141.111xE^2 + 36724.7xE^3 & E \leq 0.2 \text{ MeV} \\ 0.07387 + 10.7762\ xE - 50.5997xE^2 + 258.112xE^3 & E \leq 0.75 \text{ MeV} \\ 0.17984 + 6.95545\ xE + 1.39815xE^2 + 0.34241xE^3 & E \leq 10.0 \text{ MeV} \end{cases}$$

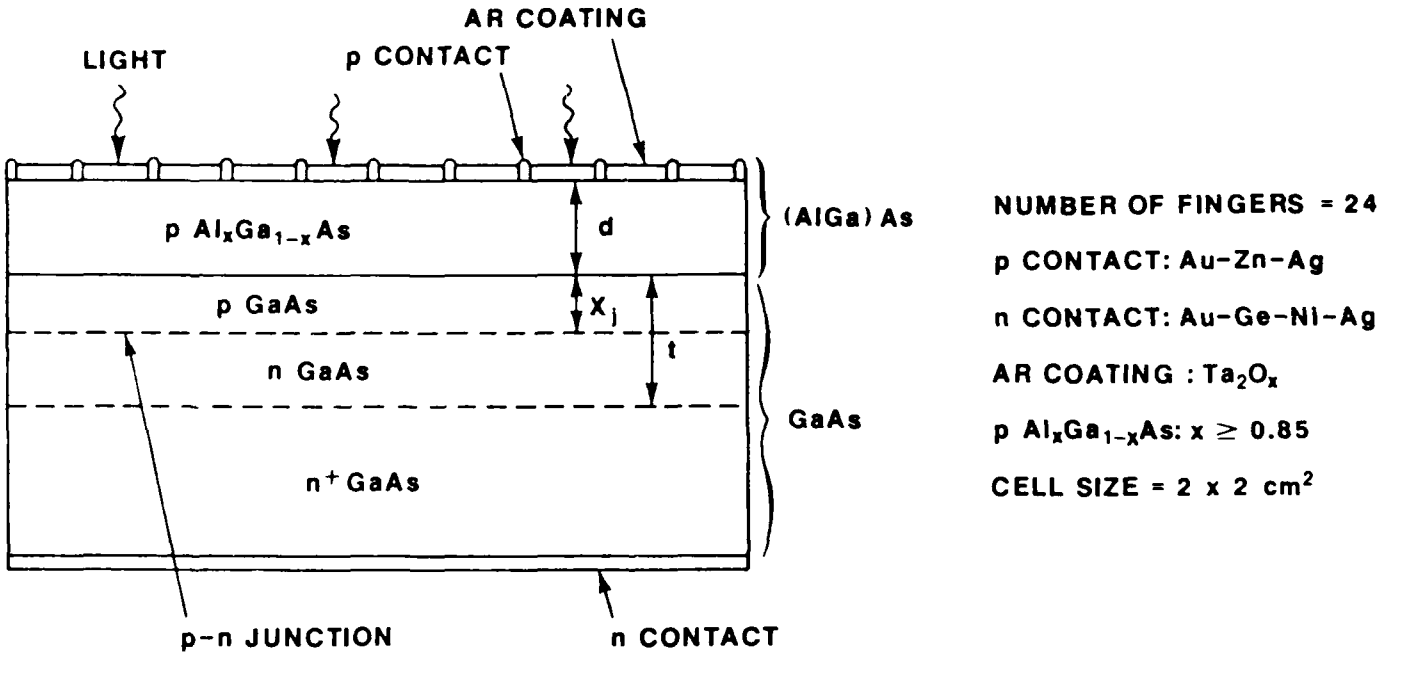

Fig. 1.1. The cross section view of an (AlGa)As-GaAs p-n junction solar cell.

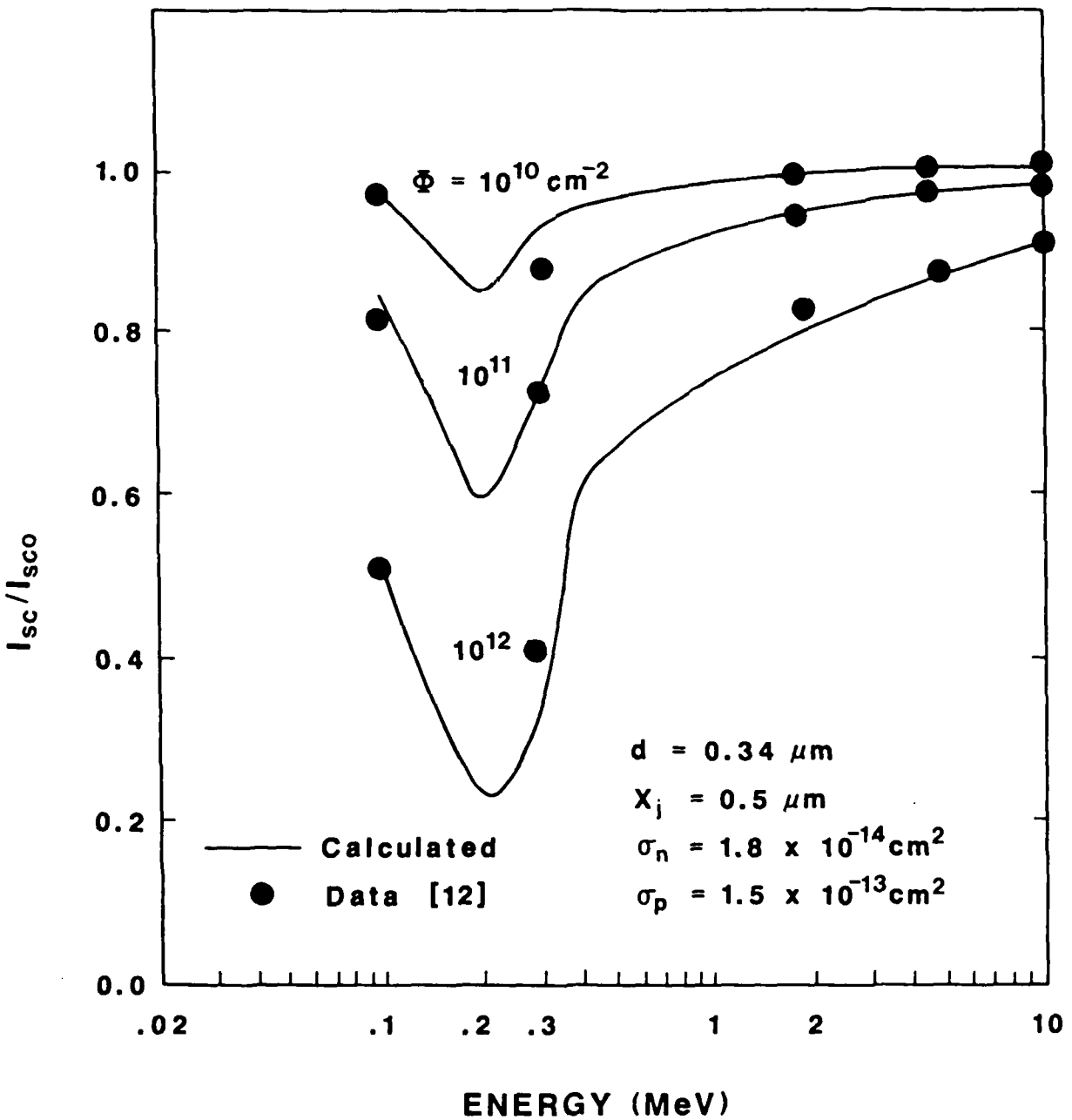

Fig. 1.2. The calculated I_{sc} degradation ratio in the proton-irradiated $Al_{0.85}Ga_{0.15}$-GaAs single-junction solar cell. Solid curves are from our calculations, solid dots are the experimental data.

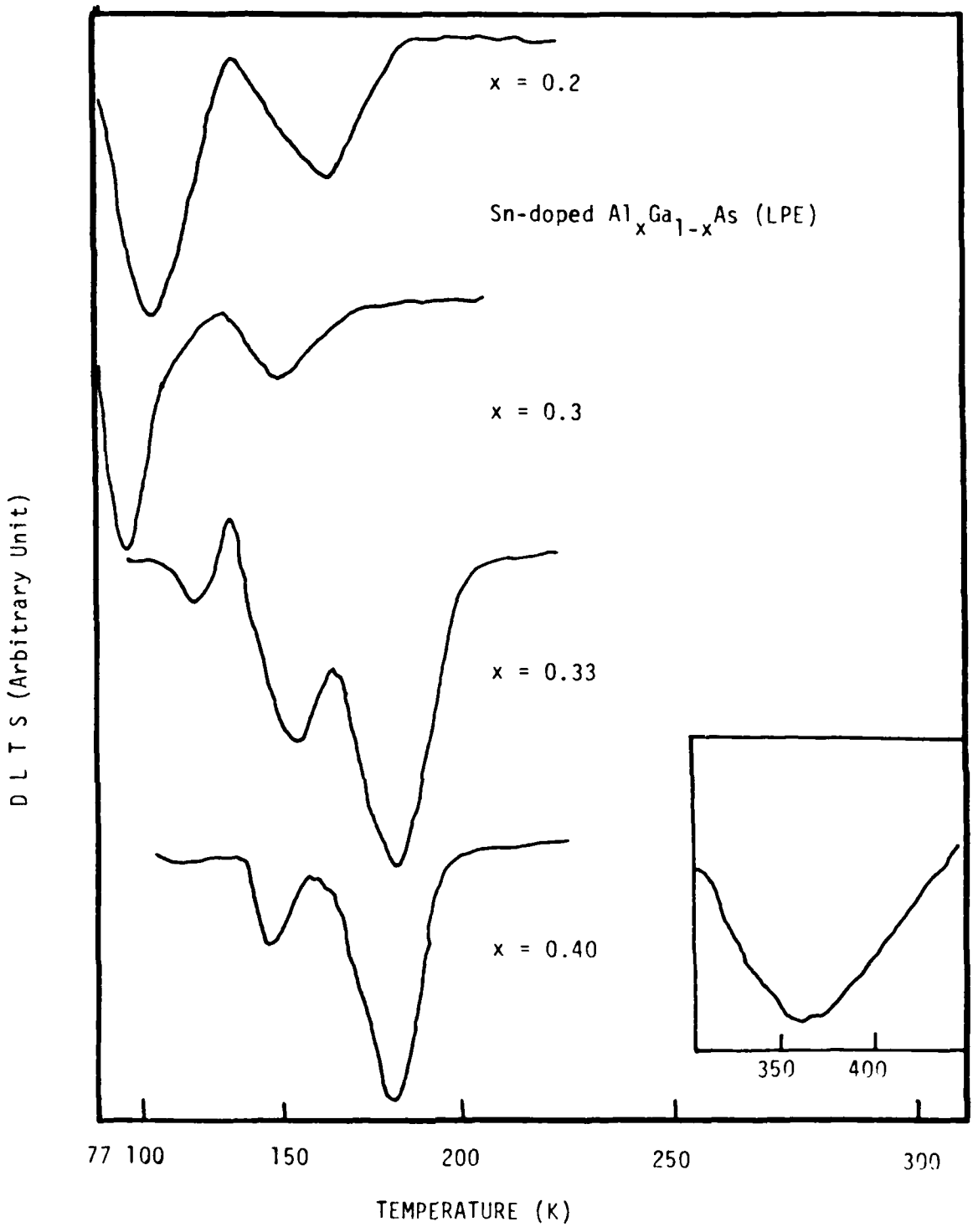

Fig. 2.1. Variation of DLTS spectra versus Aluminium contents

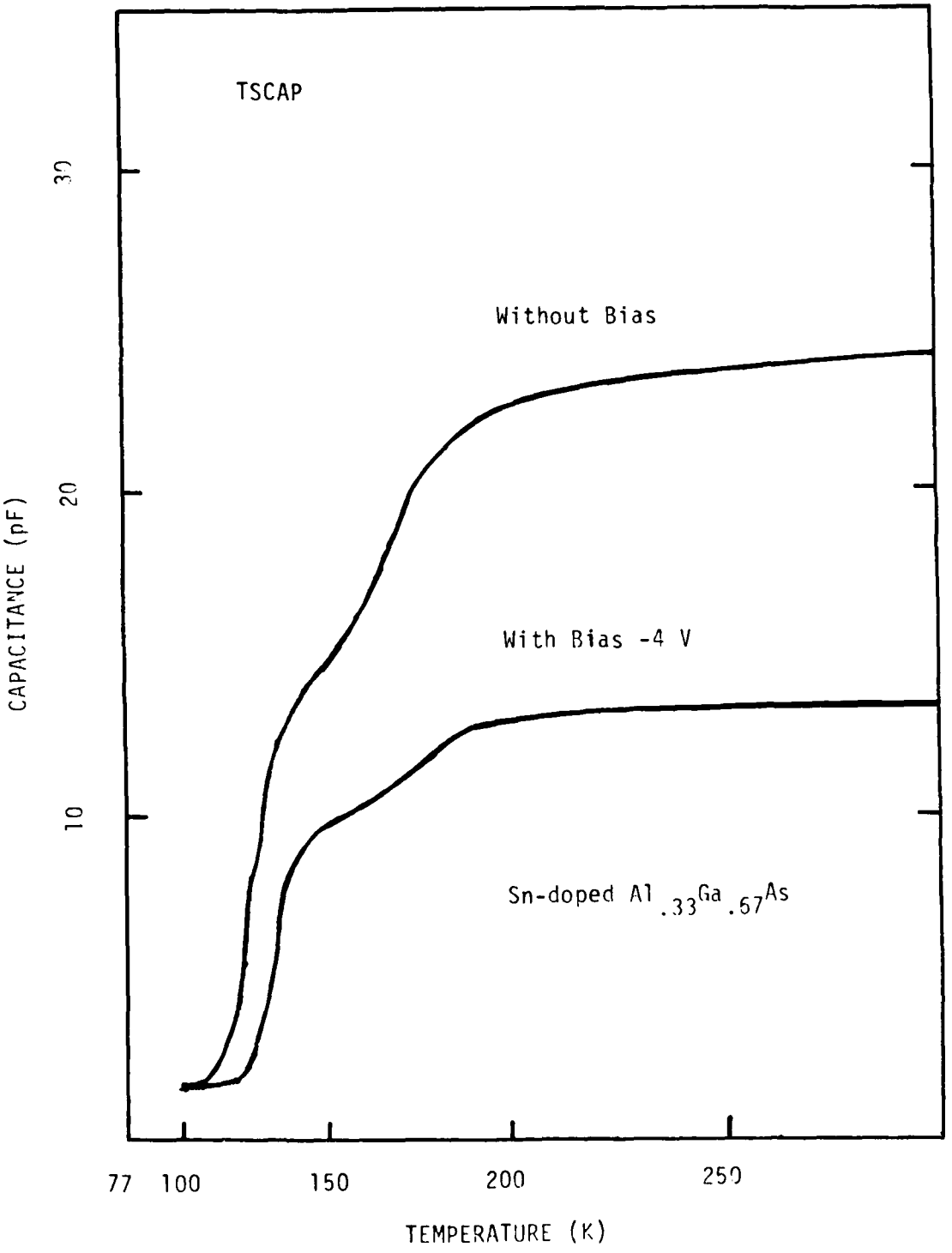

Fig. 2.2. TSCAP spectra of the Sn-doped $Al_{0.33}Ga_{0.67}As$

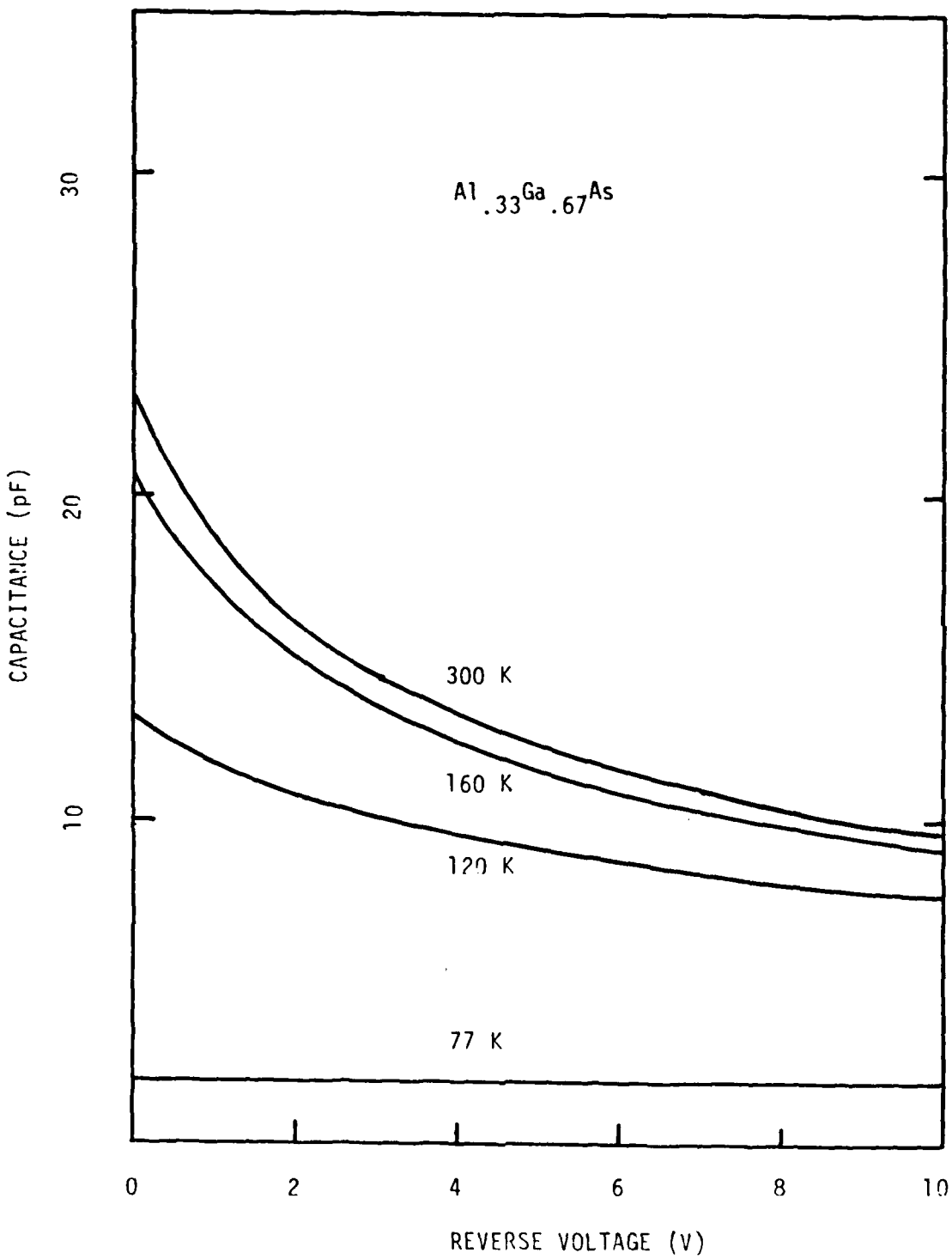

Fig. 2.3. Constant temperature capacitance-voltage curves of $Al_{\emptyset.33}Ga_{\emptyset.67}As$

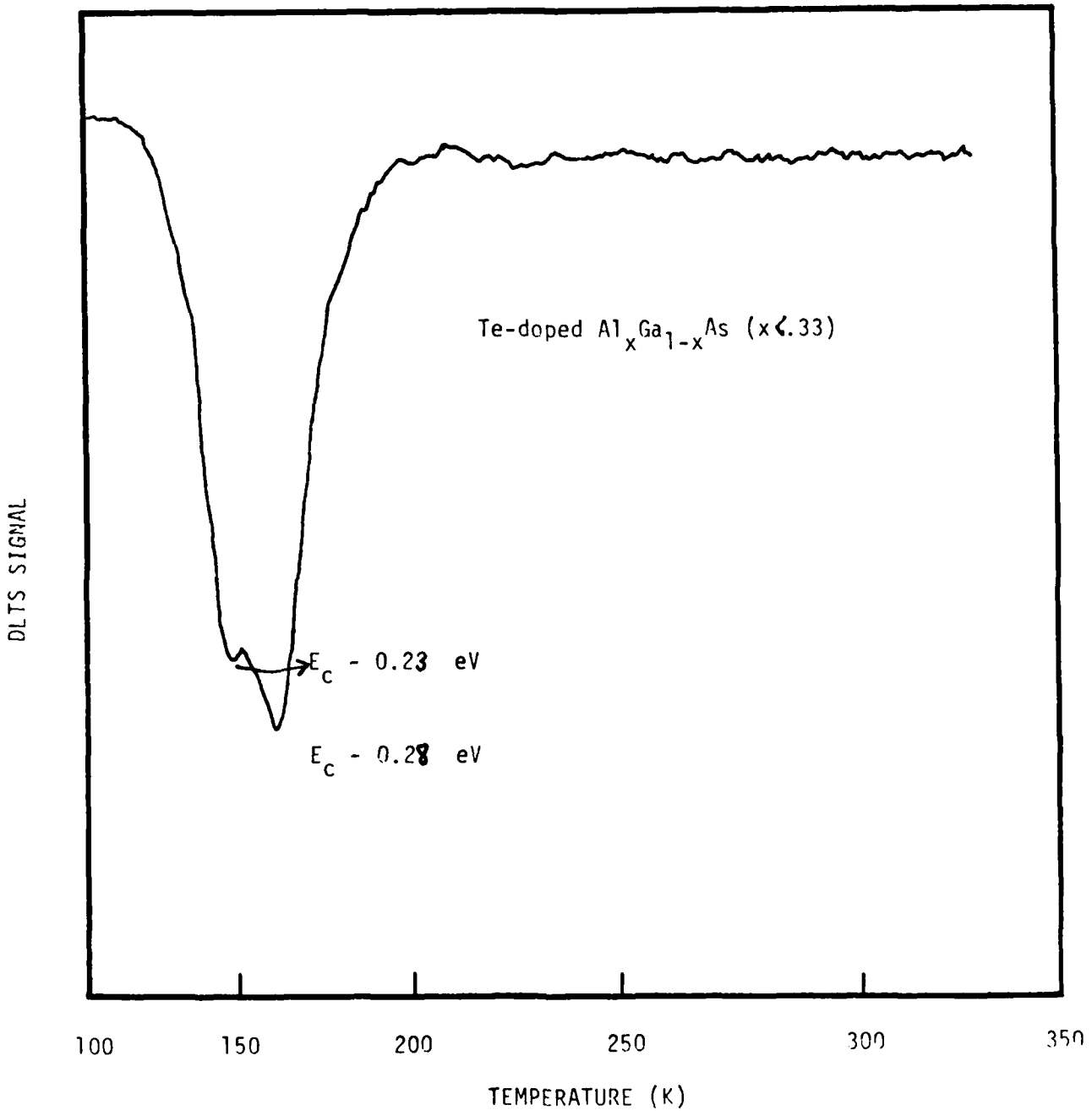

Fig. 2.4. DLTS spectrum of the 1-MeV electron irradiated Te-doped $Al_xGa_{1-x}As$ (Ø.3<x<Ø.33)

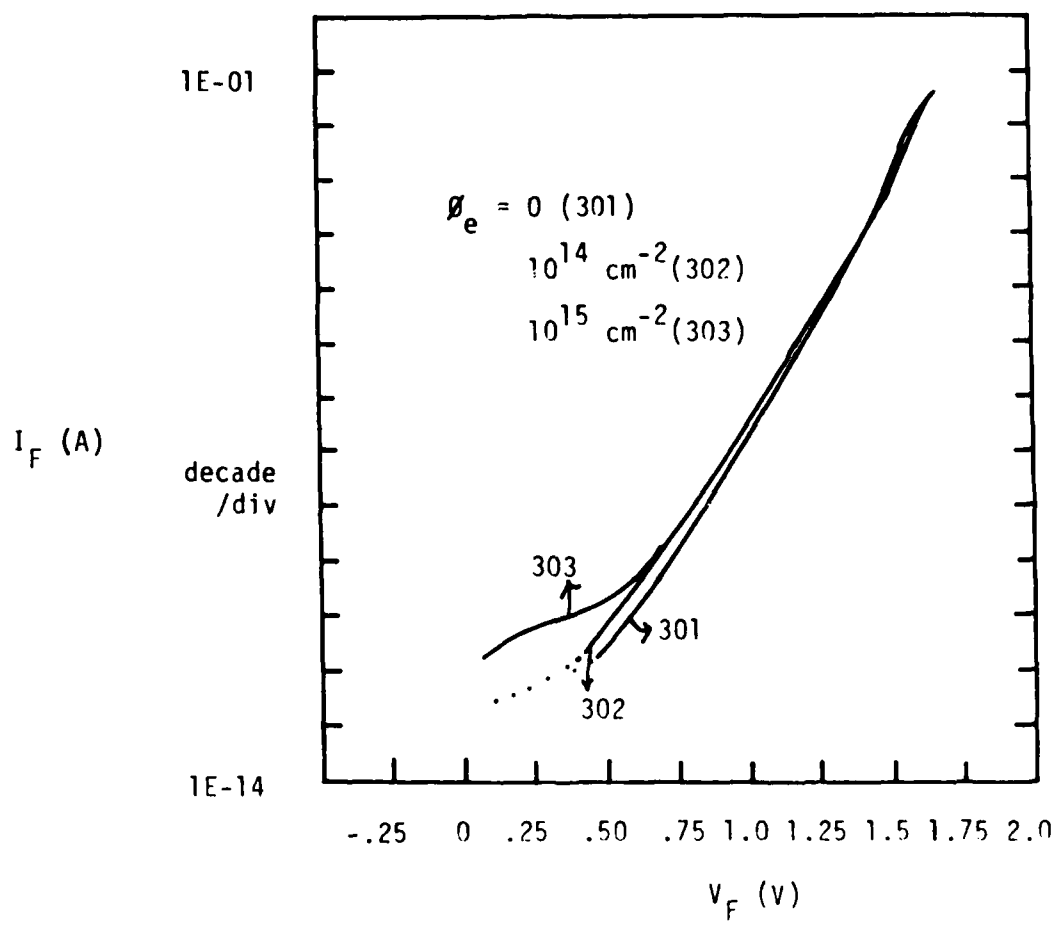

Fig. 2.5. Current-voltage characteristics of the 1-MeV electron irradiated $Al_xGa_{1-x}As$

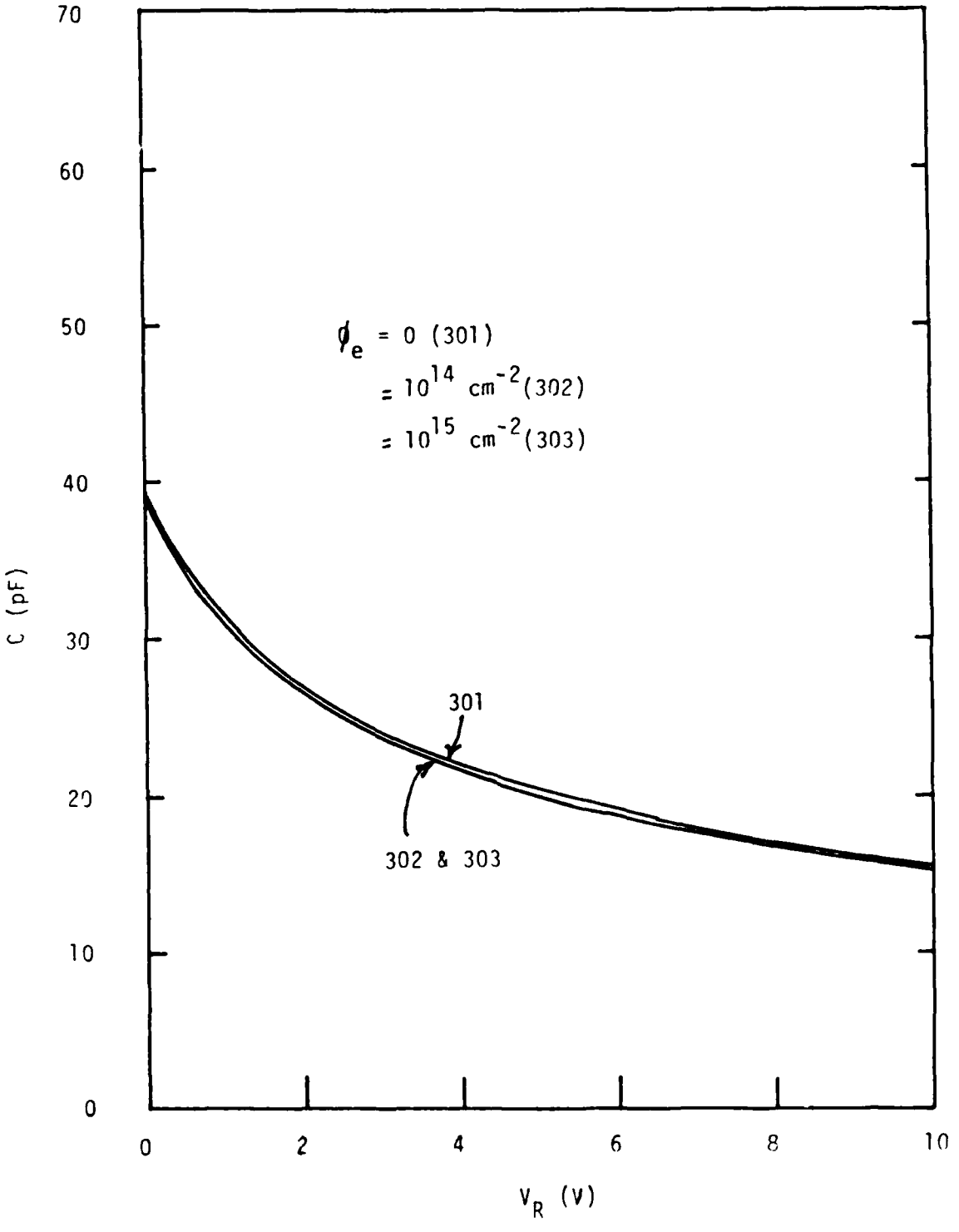

Fig. 2.6. Capacitance-voltage characteristics of the 1-MeV electron irradiated $Al_xGa_{1-x}As$ (Ø.3<x<Ø.33)

Table 1.1. Values of input parameters for calculating the damage constants of minority carrier diffusion lengths in the proton irradiated $Al_{0.85}Ga_{0.15}As/GaAs$, $Al_{0.85}Ga_{0.15}As/Al_{0.35}Ga_{0.65}As$ single junction and $Al_{0.35}Ga_{0.65}As/GaAs/In_{0.53}Ga_{0.47}As$ triple junction solar cells.

GaAs	AlGaAs	InGaAs
τ_o = 2 x 10^{-8} s	1 x 10^{-8}	5 x 10^{-9}
L_n = 6.0 um	4.56	7.2
L_p = 3.0	1.61	1.61
D_n = 18 cm^2 / s	20.8	103
D_p = 4.5	2.59	5
N_A = 2 x 10^{18} cm^{-3}	2 x 10^{18}	2 x 10^{18}
N_D = 1 x 10^{17}	1 x 10^{17}	1 x 10^{17}
n_i = 1.8 x 10^6 cm^{-3}	166	2.65 x 10^9
A = 4 cm^2	4	4
X_j = 0.5 um	0.3	0.5
t_j = 300 um	20	15
σ_n = 1.8 x 10^{-14} cm^2	5 x 10^{-16}	5 x 10^{-16}
σ_p = 1.5 x 10^{-13} cm^2	5 x 10^{-15}	5 x 10^{-15}
T_d = 9.5 eV	10.7	8.49

Table 1.2. Values of input parameters for calculating the I_{sc} degradation in the proton irradiated $Al_{0.85}Ga_{0.15}As$-$Al_{0.40}Ga_{0.60}As$ single junction or $Al_{0.40}Ga_{0.60}As$-GaAs two junction solar cells.

Window layer depth	Junction depth	Cell thickness	Capture Cross section Proton Irradiated	
W_j (um)	X_j (um)	d_j (um)	σ_n (cm^2)	σ_p (cm^2)
Top A: 0.3	0.5	2	$5x10^{-16}$	$5x10^{-15}$
Top B: 0.3	0.5	5	$5x10^{-16}$	$5x10^{-15}$
Bottom 0.3	0.5	10	$1.8x10^{-14}$	$1.5x10^{-13}$

Table 1.3. Calculated results of the I_{sc} degradation in the proton irradiated $Al_{0.85}Ga_{0.15}As$-$Al_{0.40}Ga_{0.60}As$ single junction solar cell.

Energy (proton)	I_{sc} / I_{sco} Top A			Top B		
	10^{10}	10^{11}	10^{12}	10^{10}	10^{11}	10^{12} (p/cm^2)
100 KeV	0.993	0.969	0.829	0.993	0.969	0.829
200 KeV	0.991	0.960	0.828	0.991	0.960	0.828
300 KeV	0.992	0.963	0.832	0.992	0.963	0.832
400 KeV	0.996	0.992	0.963	0.994	0.981	0.917
1 MeV	0.996	0.994	0.980	0.996	0.993	0.968
2 MeV	0.996	0.995	0.984	0.996	0.994	0.974
5 MeV	0.996	0.969	0.987	0.996	0.994	0.980
10 MeV	0.996	0.996	0.992	0.996	0.995	0.989

Table 1.4. Calculated results of the I_{sc} degradation in the proton irradiated $Al_{0.40}Ga_{0.60}As$-GaAs two junction solar cells.

Energy (proton)	I_{sc} / I_{sco} AlGaAs			GaAs			
	10^{10}	10^{11}	10^{12}	10^{10}	10^{11}	10^{12}	(p/cm^2)
100 KeV	0.993	0.969	0.829	1.0	1.0	1.0	
200 KeV	0.991	0.960	0.828	1.0	1.0	1.0	
300 KeV	0.992	0.963	0.832	1.0	1.0	1.0	
400 KeV	0.996	0.992	0.963	1.0	1.0	1.0	
1 MeV	0.996	0.993	0.968	0.948	0.965	0.843	
2 MeV	0.996	0.994	0.974	0.993	0.974	0.871	
5 MeV	0.996	0.994	0.980	0.994	0.981	0.903	
10 MeV	0.996	0.995	0.989	0.995	0.988	0.941	

Table 1.5. I_{SC} degradation for the proton irradiated (AlGa)As/GaAs/(InGa)As triple junction solar cells

Energy (MeV)	Fluences (cm^{-2})	Top Cell $Al_{0.35}Ga_{0.65}As$	Middle Cell GaAs	Bottom Cell $In_{0.53}Ga_{0.47}As$
	10^{10}	0.988	1.0	1.0
0.1	10^{11}	0.953	1.0	1.0
	10^{12}	0.796	1.0	1.0
	10^{10}	0.990	1.0	1.0
0.2	10^{11}	0.969	1.0	1.0
	10^{12}	0.869	1.0	1.0
	10^{10}	0.990	1.0	1.0
0.3	10^{11}	0.971	1.0	1.0
	10^{12}	0.872	1.0	1.0
	10^{10}	0.99	0.98	1.0
2.0	10^{11}	0.99	0.95	1.0
	10^{12}	0.98	0.78	1.0
	10^{10}	0.99	0.99	1.0
5.0	10^{11}	0.99	0.97	1.0
	10^{12}	0.98	0.87	1.0
	10^{10}	0.99	0.99	0.99
10.0	10^{11}	0.99	0.97	0.99
	10^{12}	0.99	0.84	0.98

Table 1.6. Calculated damage constants of the minority-carrier diffusion lengths for GaAs single junction solar cell

Energy (MeV)	K_{Ln}	K_{Lp}
0.1	0.105	0
0.3	0.00081	0.34
1.0	0.00025	0.00835
2.0	0.00006	0.00273
5.0	0.000029	0.00169
10.0	0.000006	0.00109

Table 1.7. Calculated damage constants of the minority-carrier diffusion lengths in the proton irradiated $Al_{0.35}Ga_{0.65}As$ single junction solar cell.

Energy (MeV)	K_{Ln}	K_{Lp}
0.1	0.00093	0
0.3	0.000017	0.00161
1.0	0.000010	0.000215
2.0	0	0.000184
5.0	0	0.000049
10.0	0	0.000042

Table 1.8. Calculated damage constants of the minority-carrier diffusion lengths in the proton irradiated $Al_{0.35}Ga_{0.65}As$/GaAs/$In_{0.53}Ga_{0.47}As$ triple junction solar cells.

Energy	(AlGa)As		GaAs		(InGa)As	
(MeV)	K_{Ln}	K_{Lp}	K_{Ln}	K_{Lp}	K_{Ln}	K_{Lp}
0.1	0.00093	0	0	0	0	0
0.3	0.000017	0.00161	0	0	0	0
1.0	0.000010	0.00021	0	0	0	0
2.0	0	0.000092	0.00036	0.00035	0	0
10.0	0	0.000042	0.00081	0.00245	0	0.00000998

Table 1.9. Calculated and experimental data of degradations of I_{sc}, V_{oc} and η_c in the proton-irradiated (AlGa)As-GaAs single junction solar cells.

Energy (MeV)	Fluence (cm^{-2})	I_{sc}/I_{sco}		V_{oc}/V_{oco}		η_c/η_{co}	
		Cal.	Exp.	Cal.	Exp.	Cal.	Exp.
0.1	10^{10}	0.97	0.97	0.97	0.925	0.94	0.89
	10^{11}	0.80	0.81	0.72	0.81	0.61	0.63
	10^{12}	0.49	0.50	0.63	0.66	0.30	0.28
0.3	10^{10}	0.92	0.87	0.93	0.94	0.85	0.81
	10^{11}	0.74	0.71	0.89	0.86	0.67	0.62
	10^{12}	0.44	0.46	0.85	0.78	0.37	0.31
1.0	10^{10}	0.98	-	0.96	-	0.94	-
	10^{11}	0.95	-	0.92	-	0.88	-
	10^{12}	0.80	-	0.89	-	0.71	-
2.0	10^{10}	0.99	0.98	0.98	0.979	0.97	0.95
	10^{11}	0.96	0.938	0.96	0.94	0.93	0.90
	10^{12}	0.83	0.81	0.93	0.87	0.78	0.71
5.0	10^{10}	0.99	1.00	0.99	1.00	0.98	1.00
	10^{11}	0.97	0.93	0.96	0.97	0.93	0.90
	10^{12}	0.86	0.84	0.93	0.90	0.80	0.76
10.0	10^{10}	0.99	1.00	0.995	0.99	0.98	0.99
	10^{11}	0.97	0.96	0.975	0.97	0.945	0.95
	10^{12}	0.89	0.89	0.945	0.93	0.843	0.84

Table 1.10. Values of input parameters for calculating degradations of I_{sc} and V_{oc} and damage constants of the minority carrier diffusion lengths for one-MeV electron irradiated $Al_{0.33}Ga_{0.67}As$ single junction solar cell.

$\tau_n = 4 \times 10^{-9}$ s	$\tau_p = 4 \times 10^{-9}$
$L_n = 3.41$ um	$L_p = 0.50$
$D_n = 29.07$ cm^2/s	$D_p = 0.625$
$N_D = 1 - 2 \times 10^{17}$ cm^{-3}	$N_A = 2 \times 10^{18}$
$x_j = 0.55$ um	cell thickness = 3 - 4 um
d = 0.3 um	$\sigma_n = 2 \times 10^{-15}$ cm^2
A = 4 cm^2	$\sigma_p = 2 \times 10^{-14}$
W = 0.14 um	

Table 1.11. Calculated damage constants of the minority-carrier diffusion lengths, I_{sc}, V_{oc} and n_c degradations for one-MeV electron irradiated (AlGa)As-$Al_{0.33}Ga_{0.67}As$ single junction solar cell.

Fluence	10^{15} cm^{-2}		10^{14} cm^{-2}	
	Calculated	Experiment	Calculated	Experiment
I_{sc}/I_{sco}	92.5 %	90.48 %	98.6 %	99.7 %
V_{oc}/V_{oco}	93.4 %	96 %	99.1 %	99.6 %
η_c/η_{co}	86.3 %	84.8 %	97.7 %	94.1 %
K_{1n}	9.90×10^{-8}	-	2.34×10^{-8}	-
K_{1p}	4.30×10^{-6}	-	7.04×10^{-7}	-

Table 1.12. Values of input parameters for calculating the I_{sc} degradation for one-MeV electron irradiated $Al_{0.40}Ga_{0.60}As$-GaAs two junction solar cells.

	Window layer depth W_j (um)	Junction depth X_j (um)	Cell thickness d_j (um)	Capture Cross section Electron Irradiated σ_n	σ_p
Top A :	0.3	0.5	2	$2x10^{-15}$	$2x10^{-14}$
Top B :	0.3	0.5	5	$2x10^{-15}$	$2x10^{-14}$
Bottom	0.3	0.5	10	$4x10^{-14}$	$4x10^{-13}$

Table 1.13. Calculated results of I_{sc} degradations for one-MeV electron irradiated $Al_{0.40}Ga_{0.60}As$-GaAs two junction solar cells.

Fluence	I_{sc} / I_{sco}			
e/cm^2	Top A - Bottom		Top B - Bottom	
10^{14}	0.990	0.940	0.984	0.940
10^{15}	0.946	0.757	0.914	0.757
10^{16}	0.747	0.406	0.655	0.406

Table 2.1. Defect parameters in the Sn-doped $Al_xGa_{1-x}As$ grown by LPE

	n (at 300 K)	n (at 77 K)	E_t (eV)	N_T (cm^{-3})	σ_n (cm^{-2})
$Al_{0.2}Ga_{0.8}As$	2.92×10^{17}	2.41×10^{17}	$E_c-0.20\pm0.02$	3.10×10^{16}	8.71×10^{-17}
			$E_c-0.30\pm0.02$	9.83×10^{15}	2.56×10^{-16}
$Al_{0.3}Ga_{0.7}As$	7.01×10^{16}	1.06×10^{16}	$E_c-0.2\pm0.02$	5.70×10^{16}	8.71×10^{-17}
			$E_c-0.30\pm0.02$	7.92×10^{15}	2.56×10^{-16}
$Al_{0.33}Ga_{0.67}A$	5.91×10^{16}	0	$E_c-0.17\pm0.02$	3.93×10^{14}	1.59×10^{-15}
			$E_c-0.20\pm0.02$	3.58×10^{16}	8.71×10^{-17}
			$E_c-0.30\pm0.02$	2.43×10^{16}	2.56×10^{-16}
$Al_{0.4}Ga_{0.6}As$	9.95×10^{16}	0	$E_c-0.20\pm0.02$	7.44×10^{16}	8.71×10^{-17}
			$E_c-0.30\pm0.02$	1.59×10^{16}	2.56×10^{-16}
			$E_c-0.86\pm0.02$	4.33×10^{14}	8.12×10^{-13}

Table 2. 2. Defect parameters in Te-doped $Al_{0.3}Ga_{0.7}As$ grown by LPE

	N_D (300 K)	N_T (77K)	E_T (eV)	N_T (cm^{-3})	σ_n (cm^{-2})
$Al_{0.3}Ga_{0.7}As$	2.0×10^{17}	2.03×10^{16}	$E_c-0.33$	1.79×10^{17}	2.42×10^{-13}

Table 2.3. Summary of DLTS, I-V, and C-V Measurements on One-MeV electron Irradiated AlGaAs (33 %) Cells

ϕ_e (e/cm^2)	Ideality factor	N_D (cm^{-3})	E_t (eV)	N_t (cm^{-3})	σ_n (cm^2)	τ_n (ns)
0	2.06	1.72×10^{17}	$E_c-0.23$	1.93×10^{16}	5.88×10^{-16}	2.32
			$E_c-0.28$	1.47×10^{17}	3.86×10^{-15}	0.0463
10^{14}	2.14	1.67×10^{17}	$E_c-0.23$	1.88×10^{16}	5.88×10^{-16}	2.25
			$E_c-0.28$	1.43×10^{17}	3.86×10^{-15}	0.047
10^{15}	2.17	1.64×10^{17}	$E_c-0.23$	1.85×10^{16}	5.88×10^{-16}	2.20
			$E_c-0.28$	1.40×10^{17}	3.86×10^{-15}	0.0473

Table.2.4 Specific contact resistance for the Ge-p/n diodes

and Ge/GaAs p-n diodes fabricated by MOCVD technique.

Diodes	OM-506	OM-507	OM-514 (A)	OM-514 (B)	
R_C (Ω)	286	95.2	3.0	1.9	300 K
			4.5	3.5	77 K
E (meV)			3.56	5.53	

U.S.Government Printing Office: 1987 - 748-061/60771

END

7-87

DTIC